

REAL-TIME TRANSIENT TEMPERATURE COMPUTATION OF POWER CABLES INCLUDING MOISTURE MIGRATION MODELLING

R. John Millar and Matti Lehtonen
Helsinki University of Technology
Espoo, Finland
john.millar@hut.fi

Abstract – A conceptually simple and robust methodology for real time monitoring and transient cable rating is offered. The paper outlines a general approach suitable for a wide range of application, and also provides a specific but typical example of its implementation. The main advantage of the approach is its inherent ability to cope with changes in the thermal properties of the cable or its environment.

A major challenge, particularly with transient rating, is to incorporate moisture migration modelling, which refers to the growth of a dry zone around the cables when they exceed a critical temperature. A new approach to this problem is presented theoretically and substantiated with both simulations and measured results. In addition, seasonal changes in the nominal properties of the cable environment can be incorporated in the algorithm, which operates in real-time and is computationally light.

It is hoped that the collection of techniques embodied in the text and accompanying figures will be of interest and service to the cable rating community in the ongoing endeavour to further improve both the efficient utilisation and reliability of power system equipment.

Keywords: Cable rating, real-time monitoring, online temperature computation, underground cables, moisture migration, emergency rating

1 INTRODUCTION

There is, at present, considerable interest in applying transient rating and real-time temperature prediction techniques to underground cables in order to realise higher load transfer than is possible using steady-state calculations, for example [1]-[3]. To be fully effective, real-time algorithms should embody moisture migration modelling and, in addition, be able to cope with changing environmental parameters in cases where seasonal changes in the cable environment are significant. This paper contains a new approach to this problem.

The standards [4] are well suited to rating cables in terms of predefined load profiles, but are not directly applicable for real-time application with changing environmental parameters. This paper models both the cable and its thermal environment on a lumped parameter thermal circuit. The primary reason for doing so is that the exponential expressions that govern the step response can be conveniently converted to a real-time formulation that works in terms of hypothetical final responses based on present conditions and the previously calculated response. This means that changing thermal parameters can be directly accommodated by

appropriately changing the coefficients and time constants of the governing exponential equations at each time increment, as, contrary to previous methods, the technique is not based on the superposition of responses following an initial steady-state condition.

The following pages provide a simple theoretical framework for dealing with moisture migration and show how to embody the effects of moisture migration and seasonal changes in the nominal algorithm. The moisture migration modelling is validated by measured data from a cable scale heating tube installed in sand backfill, while finite element method (FEM) simulations are used to demonstrate the aptness of the technique for typical multiple cable configurations.

2 THE FRAMEWORK

2.1 Extending the Thermal Circuit

The foundation of this method is to represent the temperature response of a cable in its installed environment as a summation of exponential expressions, each corresponding to one loop of a thermal ladder circuit. This is, mathematically, a straightforward extension of the standard method for dealing with a cable, where the step response of a charged cable from an initial condition of zero current can be represented as:

$$\theta_m(t) = W_c \left[\sum_{n=1}^N T_{m,n} (1 - \exp(-t/\tau_n)) \right] + \theta_{d,m} + \theta_{amb} \quad (1)$$

where $\theta_m(t)$ is the step response at node m and W_c are the conductor losses. The coefficients $T_{m,n}$ and time constants τ_n , derived from the transfer functions of the thermal circuit, incorporate adjustment for sheath and armour losses, i.e. the thermal impedances for parts of the thermal circuit outside the sheath and armour must be respectively increased by the ratio of the sheath or armour losses to the conductor losses so these losses can be omitted from the solution process. $\theta_{d,m}$ is the contribution due to dielectric losses, assuming the cable is already charged at the beginning of the transient.

This treatment, insofar as the cable itself is concerned, accords with the standards [4]. The standard approach for buried cables is to calculate the response of a line source in a homogeneous environment and couple this response to the temperature rise across the cable via an attainment factor, which accounts for the heat stored in the cable during the early part of a transient. The approach this paper utilises, however, is to include the

entire cable environment in the ladder network, which eliminates the need for solutions to the exponential integral (involved in the classical solution for a line source) and the attainment factor. The advantages are that the resultant exponential expressions can be easily transformed into a computationally simple real-time formulation and that a node can be placed at the cable surface (physically relating to a point that represents the average temperature of the surface of the hottest cable).

The real-time formulation of (1) at time t_I is:

$$\theta_m(t_I) = \theta_{d,m} + \theta_{amb}(t_I) + \sum_{n=1}^N \theta_{m,n}(t_I) \quad (2)$$

where:

$$\begin{aligned} \theta_{m,n}(t_I) = & \theta_{m,n}(t_{I-1}) \\ & + [T_{m,n} \cdot W_c(\theta_c(t_{I-1})) - \theta_{m,n}(t_{I-1})] \\ & \cdot [1 - \exp(-(t_I - t_{I-1})/(\tau_n))] \end{aligned} \quad (3)$$

The thermal circuit must have nodes at all points of interest, which should include the cable surface and, in the case of cables with multimode fibres fitted for distributed temperature sensing, the point where the fibre is located, usually just inside the sheath, should be a node. For buried cables, 3 loops are generally adequate to cover the environment.

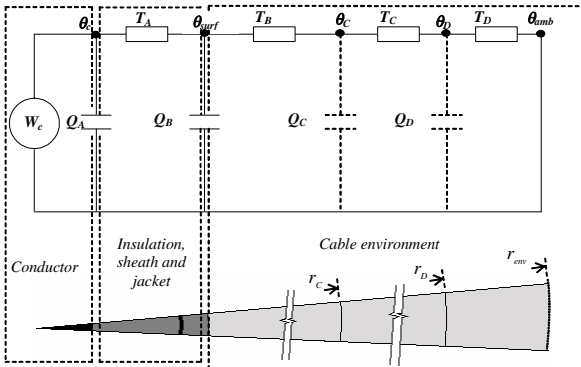


Figure 1: Thermal circuit for a cable and its thermal environment. More loops can be added for the cable if necessary.

The means to get from a thermal circuit like that shown in Figure 1 to the exponential equations in (1) is detailed in Chapter 5 and Appendix B of [5], and needs to be put into an efficient program form, as it will be necessary to recalculate the coefficients and time constants for a full range of ‘wet’ environmental parameters for a full range of critical radii (a critical radius r_x will be used to delineate the boundary between the dry and wet regions during moisture migration).

2.2 Obtaining nominal thermal circuit parameters

The objective is to obtain a set of equations that faithfully represent the transient response of the cable of concern to a constant power step in prescribed nominal conditions. This can be done in several ways, ranging from curve-fitting to a simulated response (noting that readily available FEM programs are nowadays able to deal with much more complicated installation configurations than standard analytical methods can) to fully

analytical derivations where possible. When moisture migration is an issue, the cable and the region around the cable must be treated analytically, in order to implement the modelling detailed in this paper. A fully analytical method for deriving a thermal circuit from a directly buried cable in a homogeneous environment is summarised below.

2.2.1 An Equivalent Cylindrical Environment

The nominal thermal resistance of the environment $T_{4,nom}$ (in terms of a single-phase equivalent for multi-cable installations such as trefoil, flat touching, flat separate, etc.) must be calculated according to the steady-state standards [6] in terms of a nominal thermal resistivity, ρ_{nom} .

The cylindrical environment should be based on a single-cable equivalent, which means the cylindrical environment has a thermal resistivity of $k_{conv}\rho_{nom}$, where the conversion factor k_{conv} represents the ratio of the external equivalent thermal resistance of a single cable in its multi-cable installed configuration to the thermal resistance of a single cable (on its own) in the same semi-infinite environment.

$$k_{conv} = \frac{T_{4,nom}}{(\rho_{nom}/2\pi)\ln(u + \sqrt{u^2 - 1})} \quad (4)$$

where u is the burial depth L divided by the external radius of one cable, r_e . Equation (4) simply scales up the thermal resistivity of the cable environment to account for the omission of the other cables (which have the same losses) in the single cable representation.

Figure 2 illustrates the procedure.

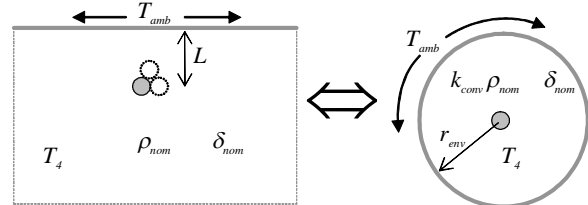


Figure 2: Single-phase cylindrical representation of a trefoil cable installation

The external thermal resistance in terms of the equivalent cylindrical representation is:

$$T_{4,nom} = \frac{k_{conv}\rho_{nom}}{2\pi} \ln\left(\frac{r_{env}}{r_e}\right) \quad (5)$$

Solving (4) and (5) gives:

$$r_{env} = r_e \left(u + \sqrt{u^2 - 1} \right) \quad (6)$$

The environmental part of the thermal circuit should consist of three loops (or perhaps four, if the cables are very small). The radius of each corresponding region in the equivalent cylindrical environment should split the external thermal resistance into equal parts, so for three loops, referring to Figure 1:

$$r_C = r_e \left(\frac{r_{env}}{r_e} \right)^{1/3} \quad (7)$$

and

$$r_D = r_e \left(\frac{r_{env}}{r_e} \right)^{2/3} \quad (8)$$

The thermal capacitances of the environment can be lumped to the radial nodes, at r_e , r_C and r_D assuming a logarithmic temperature distribution, i.e. extending the logic employed by Van Wormer in dividing the internal thermal capacitances of the cable itself [7].

Using Van Wormer's 'modified equivalent π circuit',

$$p(r_o, r_i) = \frac{1}{2 \ln \left(\frac{r_o}{r_i} \right)} - \frac{1}{\frac{r_o^2}{r_i^2} - 1} \quad (9)$$

where r_o is the outside and r_i the inside nodal radius of the section in question. The proportion of the capacitance allocated to the node at the inside radius of each region is $p \cdot \pi (r_o^2 - r_i^2) / (k_{conv} \rho_s \delta_s (1 + \lambda_1 + \lambda_2))$ with the remainder being added to the node at the outside radius of the region. The sheath and armour loss factors, λ_1 and λ_2 , are present in the denominator because, as mentioned in section 2.1, the algorithm works in terms of the conductor losses only. Note that the final thermal capacitance in the cable part of the thermal circuit, which is normally omitted to facilitate the derivation of a transfer function, is added to the first thermal capacitance of the environment. The final capacitance component associated with the outermost node at r_{env} is omitted when calculating the transfer functions for the nodal responses that are of interest.

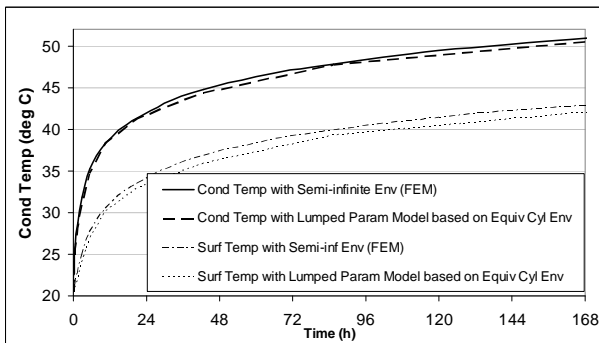


Figure 3: Comparison of a full FEM model with a lumped parameter analysis using the equivalent cylindrical environmental model for the constant loss step response of the hottest cable in a HV trefoil installation

Figure 3 shows the simulated responses of a cable in a semi-infinite environment (well almost, the FEM simulation used has a thermal field 50 x 35 m), and a step response consistent with the lumped parameter circuit shown in Figure 1.

The losses are held constant in all cases, so as to obtain a pure step response. In the real-time algorithm

comprising (2) and (3), the losses are calculated according to the calculated temperatures (and measured current) at every time increment.

We now have a continuous thermal model of a cable installation from the hottest conductor to a symbolic outer radius r_{env} , which may be considered an isotherm at ambient temperature, θ_{amb} . Because both the cable and the region around the cable are accurately modelled, and because the thermal resistance of the equivalent cylindrical environment corresponds to the thermal resistance of the actual semi-infinite environment, we can assume that the short-term and extremely long-term thermal response of the cable will be faithfully represented by the seemingly simplistic 'equivalent cylindrical modelling'. The fact that the method gives rise to slight medium term error is unavoidable when reducing semi-infinite reality to a finite cylindrical equivalent, but fortunately this is of little consequence concerning the accuracy of a real-time algorithm that redefines the hypothetical steady state towards which the response is heading every few minutes or so.

Thus we come to the crux of this paper, which concerns how to change the time constants and coefficients in (3) to reflect changes in the cable environment.

3 AN UNSTABLE ENVIRONMENT

It is assumed that seasonal changes, due to rainfall and ground water level, will affect the entire cable environment, whereas moisture migration caused by the load in the cable will affect only the region close to the cable. We will base the moisture migration analysis on traditional 2-zone modelling, but as will be shown, the modelling can be 'tuned' to a more sophisticated modelling to allow for slower return of moisture to the cable vicinity, and, if necessary, slower than instantaneous migration of the moisture away from the cable when the cable environment reaches the critical temperature for moisture migration. It is assumed that dry means dry, i.e. the thermal resistivity for a given cable environment in dry conditions, ρ_{dry} , is fixed, and that there is a unique relationship, for a given installation, between the thermal resistivity and diffusivity of the material in the cable's immediate vicinity. This should ideally be derived specifically for the backfill material in installed conditions tested from fully saturated to completely dry. In the absence of such information, Neher's empirical formula, (10), [8] can be used for most crushed rock and sand backfills, given that the thermal resistivity is the most sensitive parameter in an underground cable installation (i.e. some inaccuracy in the computation of the thermal diffusivity is acceptable; diffusivity values are probably somewhat higher than (10) predicts).

$$\delta(\rho) = 4.68 \cdot 10^{-7} / \rho^{0.8} \text{ m}^2/\text{s} \quad (10)$$

3.1 Moisture migration modelling

As stated, the moisture migration modelling is based on a transient implementation of the 2-zone method used

in the standards for steady-state rating, Amendment 3, [4].

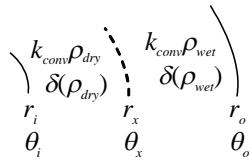


Figure 4: 2-zone moisture migration

Referring to Figure 4, the method for tracking the critical radius for moisture migration r_x , which designates the location of the critical temperature for moisture migration θ_x , assumes that if r_x lies between nodes at r_i and r_o , then the temperature profile between r_i and r_x , and between r_x and r_o , is logarithmic. The actual temperature profile is close to what would prevail in steady-state conditions, scaled to match the actual nodal temperatures calculated at each time increment. The logarithmic assumption will slightly overestimate r_x in the early part of a transient during heating and slightly underestimate r_x during cooling. On the other hand, it must be admitted that the single cable representation of a trefoil or flat configuration where the cables are touching or nearly touching is based on the average temperature of the surface of the hottest cable and, physically, moisture migration will be initiated near the points where the cables are touching slightly earlier than when the average surface temperature reaches θ_x . This means that the temperature response of a cable in a trefoil or flat touching configuration will be slightly underestimated at the onset of moisture migration, but as the migration develops, the error goes in the conservative direction, because of the logarithmic temperature distribution assumption, and because the moisture migration is physically only occurring in the direction unshielded by the adjacent cables.

Assuming a logarithmic temperature distribution, the ratio of the temperature difference between the inner node and the critical isotherm and the total temperature drop between the inner and outer nodes is:

$$\frac{\theta_i - \theta_x}{\theta_i - \theta_o} = \frac{\frac{k_{conv}\rho_{dry}}{2\pi} \ln\left(\frac{r_x}{r_i}\right)}{\frac{k_{conv}\rho_{dry}}{2\pi} \ln\left(\frac{r_x}{r_i}\right) + \frac{k_{conv}\rho_{wet}}{2\pi} \ln\left(\frac{r_o}{r_x}\right)} \quad (11)$$

In a real time formulation, we can designate $r_{x,\infty}$ as the position the critical isotherm is tending to at time t_I in terms of the calculated nodal temperatures at the previous time increment t_{I-1} .

$$r_{x,\infty}(t_I) = r_i \exp\left(\frac{\ln\left(\frac{r_o}{r_i}\right)}{1 + \frac{\rho_{dry}}{\rho_{wet}} \left(\frac{\theta_o(t_{I-1}) - \theta_x}{\theta_x - \theta_i(t_{I-1})}\right)}\right) \quad (12)$$

Incorporating (12) directly into the final algorithm would imply that the material around the cable instantly

dries out when the temperature reaches θ_x during heating and instantly rewets when the temperature returns to θ_x during cooling. The first assumption is conservative but the latter is dangerous because, especially in dry seasonal conditions, moisture can take a lot longer to return to a cable environment than it takes to leave, [9]. It is therefore advisable to control the movement of the critical radius, and this is done using (13).

$$r_x(t_I) = r_x(t_{I-1}) + (r_{x,\infty}(t_I) - r_x(t_{I-1})) \begin{cases} 1 - \exp\left(-\frac{t_I - t_{I-1}}{\tau_{mm,heating}}\right) & \text{if } r_{x,\infty}(t_I) \geq r_x(t_{I-1}) \\ 1 - \exp\left(-\frac{t_I - t_{I-1}}{\tau_{mm,cooling}}\right) & \text{if } r_{x,\infty}(t_I) < r_x(t_{I-1}) \end{cases} \quad (13)$$

If the moisture migration time constant for cooling $\tau_{mm,cooling}$ is set high, the return of moisture to the cable environment is effectively slowed down, which is an important feature of this algorithm. The slowing down of moisture movement when cables are located in back-filled concrete trenches can also be accommodated with the time constants in (13).

Thus, values for the time constants (and θ_x) depend on local installation conditions, soil conditions and moisture content. The prevailing moisture content depends on ground water levels, rainfall patterns and so on. We are gradually arriving at suitable time constant values for cable installation conditions in southern Finland, but it would be foolhardy to generalise our findings at this stage. For a more sophisticated modelling of moisture migration, more than one exponential expression can be used in (13) if so desired. It is as well to be conservative when modelling moisture migration...

3.2 The effect of moisture migration on the thermal capacitances and resistances in the thermal circuit

3.2.1 Subdividing the thermal capacitance when the critical isotherm is situated between two nodes

To investigate the shifting of thermal capacitance during moisture migration, the logarithmic approach used in section 2.2.1 to divide the capacitances in a stable environment will be extended to cover a cable environment subject to moisture migration.

Consider the region around a cable containing the critical isotherm at radius r_x that delineates the boundary between dry and wet zones. The inner and outer nodal radii of the region are r_i and r_o , as shown in Figure 4.

The assumption, validated by simulations, is that the temperature distribution during a transient will be proportional to the steady state temperature distribution, i.e. for $r_i \leq r < r_x$ the steady-state temperature distribution is:

$$\theta_r = \theta_x + W_t \frac{k_{conv}\rho_{dry}}{2\pi} \ln\left(\frac{r_x}{r}\right) \quad (14)$$

and

$$\theta_i = \theta_x + W_t \frac{k_{conv}\rho_{dry}}{2\pi} \ln\left(\frac{r_x}{r_i}\right) \quad (15)$$

For $r_x \leq r < r_o$,

$$\theta_r = \theta_x - W_t \frac{k_{conv} \rho_{wet}}{2\pi} \ln\left(\frac{r}{r_x}\right) \quad (16)$$

and

$$\theta_o = \theta_x - W_t \frac{k_{conv} \rho_{wet}}{2\pi} \ln\left(\frac{r_o}{r_x}\right) \quad (17)$$

If p_{mm} is the amount of heat capacity apportioned to the inner radius r_i , then matching the heat storage on each side of the thermal section (for the convenience of a lumped parameter treatment) to that which is really stored over the whole section means that:

$$\begin{aligned} p_{mm} \left[\pi (r_x^2 - r_i^2) q_{dry} + \pi (r_o^2 - r_x^2) q_{wet} \right] \theta_i \\ + (1 - p_{mm}) \left[\pi (r_x^2 - r_i^2) q_{dry} + \pi (r_o^2 - r_x^2) q_{wet} \right] \theta_o \\ = q_{dry} \int_{r_i}^{r_x} \theta_r 2\pi r dr + q_{wet} \int_{r_x}^{r_o} \theta_r 2\pi r dr, \end{aligned} \quad (18)$$

where q_{dry} and q_{wet} refer to the volumetric heat capacities of the dry and wet sections respectively. Substituting (14)-(17) into (18), integrating, and noting that $q = 1/\rho\delta$ gives:

$$\begin{aligned} p_{mm}(\theta_o, r_i, r_x) = \\ 0.5 \frac{\left(r_x^2 - r_o^2 + \frac{\delta_{wet}}{\delta_{dry}} (r_i^2 - r_x^2) \right) + \left(r_x^2 + \frac{\rho_{wet} \delta_{wet}}{\rho_{dry} \delta_{dry}} (r_i^2 - r_x^2) \right) \ln\left(\frac{r_o}{r_x}\right) + \frac{\delta_{wet}}{\delta_{dry}} r_i^2 \ln\left(\frac{r_x}{r_i}\right)}{\left(r_x^2 - r_o^2 + \frac{\rho_{wet} \delta_{wet}}{\rho_{dry} \delta_{dry}} (r_i^2 - r_x^2) \right) \left(\ln\left(\frac{r_o}{r_x}\right) + \frac{\rho_{dry}}{\rho_{wet}} \ln\left(\frac{r_x}{r_i}\right) \right)} \end{aligned} \quad (19)$$

Equation (9) can be used instead of (19) if the inter-nodal region under consideration is homogeneous, i.e. either totally wet or totally dry. If the region contains the critical isotherm, then (19) is used to subdivide the total thermal capacitance of that section to each node.

3.2.2 A suitable upper limit for r_x

A suitable upper limit for the critical radius can be calculated from a steady-state analysis, which, in terms of the maximum total losses from one cable, $W_{t,max}$, yields:

$$r_{x,max} = r_e \cdot e^{2\pi \left(\frac{T_{4,wet} W_{t,max} - \Delta\theta_x}{k_{conv} \rho_{wet} W_{t,max}} \right)} \quad (20)$$

which implies that the critical radius under steady-state conditions is independent of the dry parameters of the cable environment.

It may be more practical to project the maximum radius in terms of temperatures only, i.e. the maximum likely surface temperature of the cable $\theta_{e,max}$, the minimum critical temperature rise above ambient $\Delta\theta_{x,min}$ and ambient temperature $\theta_{amb,min}$, and the highest seasonal wet thermal resistivity, $\rho_{wet,max}$, in which case:

$$r_{x,max} = r_e \left(\frac{r_{env}}{r_e} \right)^{1/\left(1 + \frac{\rho_{dry}}{\rho_{wet,max}} \left(\frac{\Delta\theta_{x,min}}{(\theta_{e,max} - \theta_{amb,min}) - \Delta\theta_{x,min}} \right) \right)} \quad (21)$$

3.2.3 Calculating the parameters of the thermal circuit for a full range of critical radii and seasonal conditions

We will illustrate the calculation of thermal resistances and the allocation of thermal capacitances with a buried cable in a homogeneous environment that suits the analysis outlined in section 2, although the general method is by no means limited to such an installation. Referring to Figure 1, the calculations in (24) to (41) are performed, for a given cable installation, $u \times v$ times, for a full range of wet thermal resistivities $(\rho_{wet})_u$ at each critical radius, $(r_x)_v$. The corresponding diffusivity values, $\delta((\rho_{wet})_u)$, are calculated using (10) or an equation tailor-made for the backfill/native soil in question.

The thermal properties of the cable itself are independent of changes in the environment. The crude single-loop analysis in (22) and (23) can be substituted by a more accurate multi-loop standard cable analysis if required [4].

$$(Q_A)_{u,v} = Q_c + p(r_e, r_c) \left(Q_i + \frac{Q_s + Q_j}{1 + \lambda_1} \right) \quad (22)$$

and

$$(T_A)_{u,v} = T_1 + T_3(1 + \lambda_1) \quad (23)$$

where Q_c , Q_i , Q_s and Q_j are the thermal capacitances of the conductor, insulation, sheath and jacket. T_1 and T_3 refer to the thermal resistances of the insulation and jacket. λ_1 represents the ratio of sheath to conductor losses, the sheath loss factor. This cable has no armour.

The rest of the circuit parameters are dependent on the prevailing wet conditions of the environment, which may have a strong seasonal variation, and the position of the critical isotherm, r_x , if moisture migration is occurring. Calculation of the remaining capacitances and resistances proceeds as follows:

If $(r_x)_v = r_e$,

$$(Q_B)_{u,v} = (1 - p(r_e, r_c)) \left(Q_i + \frac{Q_s + Q_j}{1 + \lambda_1} \right) + \frac{p(r_B, r_e)}{k_{conv}(1 + \lambda_1)} \cdot \frac{\pi(r_B^2 - r_e^2)}{(\rho_{wet})_u \delta((\rho_{wet})_u)} \quad (24)$$

$$(T_B)_{u,v} = \frac{k_{conv}(1 + \lambda_1)(\rho_{wet})_u \ln\left(\frac{r_B}{r_e}\right)}{2\pi} \quad (25)$$

$$(Q_C)_{u,v} = \frac{(1 - p(r_B, r_e)) \left(\frac{\pi(r_B^2 - r_e^2)}{(\rho_{wet})_u \delta((\rho_{wet})_u)} \right)}{k_{conv}(1 + \lambda_1)} + \frac{p(r_C, r_B)}{k_{conv}(1 + \lambda_1)} \cdot \frac{\pi(r_C^2 - r_B^2)}{(\rho_{wet})_u \delta((\rho_{wet})_u)} \quad (26)$$

$$(T_C)_{u,v} = \frac{k_{conv}(1 + \lambda_1)(\rho_{wet})_u \ln\left(\frac{r_C}{r_B}\right)}{2\pi} \quad (27)$$

$$(Q_D)_{u,v} = \frac{(1-p(r_C, r_B))}{k_{conv}(1+\lambda_1)} \left(\frac{\pi(r_C^2 - r_B^2)}{(\rho_{wet})_u \delta((\rho_{wet})_u)} \right) + \frac{P(r_{env}, r_C)}{k_{conv}(1+\lambda_1)} \cdot \frac{\pi(r_{env}^2 - r_C^2)}{(\rho_{wet})_u \delta((\rho_{wet})_u)} \quad (28)$$

$$(T_D)_{u,v} = \frac{k_{conv}(1+\lambda_1)(\rho_{wet})_u}{2\pi} \ln \left(\frac{r_{env}}{r_C} \right) \quad (29)$$

If $r_B < (r_x)_v \leq r_C$, (27), (28) and (29) still apply for T_C , Q_D and T_D , but for the rest of the circuit parameters:

$$(Q_B)_{u,v} = (1-p(r_e, r_c)) \left(Q_i + \frac{Q_s + Q_j}{1+\lambda_1} \right) + \frac{p_{mm}(r_B, r_e, (r_x)_v, (\rho_{wet})_m)}{k_{conv}(1+\lambda_1)} \left[\frac{\pi((r_x)_v^2 - r_e^2)}{\rho_{dry} \delta(\rho_{dry})} + \frac{\pi(r_B^2 - (r_x)_v^2)}{(\rho_{wet})_u \delta((\rho_{wet})_u)} \right] \quad (30)$$

$$(T_B)_{u,v} = \frac{k_{conv}(1+\lambda_1)}{2\pi} \left[\rho_{dry} \ln \left(\frac{(r_x)_v}{r_e} \right) + (\rho_{wet})_m \ln \left(\frac{r_B}{(r_x)_v} \right) \right] \quad (31)$$

$$(Q_C)_{u,v} = \frac{(1-p_{mm}(r_B, r_e, (r_x)_v, (\rho_{wet})_m))}{k_{conv}(1+\lambda_1)} \left[\frac{\pi((r_x)_v^2 - r_e^2)}{\rho_{dry} \delta(\rho_{dry})} + \frac{\pi(r_B^2 - (r_x)_v^2)}{(\rho_{wet})_u \delta((\rho_{wet})_u)} \right] + \frac{P(r_C, r_B)}{k_{conv}(1+\lambda_1)} \cdot \frac{\pi(r_C^2 - r_B^2)}{(\rho_{wet})_u \delta((\rho_{wet})_u)} \quad (32)$$

If $r_B < (r_x)_v \leq r_C$, (29) is still valid for T_D , but for the rest:

$$(Q_B)_{u,v} = (1-p(r_B, r_e)) \left(Q_i + \frac{Q_s + Q_j}{1+\lambda_1} \right) + \frac{P(r_B, r_e)}{k_{conv}(1+\lambda_1)} \cdot \frac{\pi(r_B^2 - r_e^2)}{\rho_{dry} \delta(\rho_{dry})} \quad (33)$$

$$(T_B)_{u,v} = \frac{k_{conv}(1+\lambda_1)}{2\pi} \rho_{dry} \ln \left(\frac{r_B}{r_e} \right) \quad (34)$$

$$(Q_C)_{u,v} = \frac{1-p(r_B, r_e)}{k_{conv}(1+\lambda_1)} \cdot \frac{\pi(r_B^2 - r_e^2)}{\rho_{dry} \delta(\rho_{dry})} + \frac{p_{mm}(r_C, r_B, (r_x)_v, (\rho_{wet})_u)}{k_{conv}(1+\lambda_1)} \left[\frac{\pi((r_x)_v^2 - r_B^2)}{\rho_{dry} \delta(\rho_{dry})} + \frac{\pi(r_C^2 - (r_x)_v^2)}{(\rho_{wet})_u \delta((\rho_{wet})_u)} \right] \quad (35)$$

$$(T_C)_{u,v} = \frac{k_{conv}(1+\lambda_1)}{2\pi} \left[\rho_{dry} \ln \left(\frac{(r_x)_v}{r_B} \right) + (\rho_{wet})_u \ln \left(\frac{r_C}{(r_x)_v} \right) \right] \quad (36)$$

$$(Q_D)_{u,v} = \frac{(1-p_{mm}(r_C, r_B, (r_x)_v, (\rho_{wet})_u))}{k_{conv}(1+\lambda_1)} \left[\frac{\pi((r_x)_v^2 - r_B^2)}{\rho_{dry} \delta(\rho_{dry})} + \frac{\pi(r_C^2 - (r_x)_v^2)}{(\rho_{wet})_u \delta((\rho_{wet})_u)} \right] + \frac{P(r_{env}, r_C)}{k_{conv}(1+\lambda_1)} \cdot \frac{\pi(r_{env}^2 - r_C^2)}{(\rho_{wet})_u \delta((\rho_{wet})_u)} \quad (37)$$

If $r_x > r_C$, (33) and (34) cover Q_B and T_B , but for the rest of the circuit parameters:

$$(Q_C)_{u,v} = \frac{1-p(r_B, r_e)}{k_{conv}(1+\lambda_1)} \cdot \frac{\pi(r_B^2 - r_e^2)}{\rho_{dry} \delta(\rho_{dry})} + \frac{p(r_C, r_B)}{k_{conv}(1+\lambda_1)} \left[\frac{\pi(r_C^2 - r_B^2)}{\rho_{dry} \delta(\rho_{dry})} \right] \quad (38)$$

$$(T_C)_{u,v} = \frac{k_{conv}(1+\lambda_1)}{2\pi} \rho_{dry} \ln \left(\frac{r_C}{r_B} \right) \quad (39)$$

$$(Q_D)_{u,v} = (1-p(r_C, r_B)) \frac{\pi((r_x)_v^2 - r_B^2)}{\rho_{dry} \delta(\rho_{dry})} + \frac{p_{mm}(r_{env}, r_C, (r_x)_v, (\rho_{wet})_u)}{k_{conv}(1+\lambda_1)} \left[\frac{\pi((r_x)_v^2 - r_C^2)}{\rho_{dry} \delta(\rho_{dry})} + \frac{\pi(r_{env}^2 - (r_x)_v^2)}{(\rho_{wet})_u \delta((\rho_{wet})_u)} \right] \quad (40)$$

$$(T_D)_{u,v} = \frac{k_{conv}(1+\lambda_1)}{2\pi} \left(\rho_{dry} \ln \left(\frac{(r_x)_v}{r_C} \right) + (\rho_{wet})_u \ln \left(\frac{r_{env}}{(r_x)_v} \right) \right) \quad (41)$$

An algorithm embodying the full range of discrete calculations from (22) to (41) giving the parameters of the thermal circuit for each $(\rho_{wet})_u$ at each $(r_x)_v$ is coupled to a subroutine that derives the coefficients and

time constants of the exponential equations governing the step response at each node of interest. All nodes up to and including the last node that bounds $r_{x,max}$ need to be included. This gives N times $u \times v$ matrices for each time constant and N times the number of nodes of interest times $u \times v$ matrices for the coefficients, where N is the number of loops in the thermal circuit (the time constants are the same for each nodal response). From this, continuous functions making every coefficient and time constant a function of wet thermal resistivity and critical radius for moisture migration can be generated, noting that it is advisable to make the functions stepwise continuous, with a step at the intermediate nodes in the cable environment.

Relationships between the time constants and critical radii, for a range of critical radii are shown in Figure 5. Only τ_1 and τ_2 are significantly affected. The reason for putting a step at the first environmental node (in this case, $r_B = 0.16$ m) can be clearly seen.

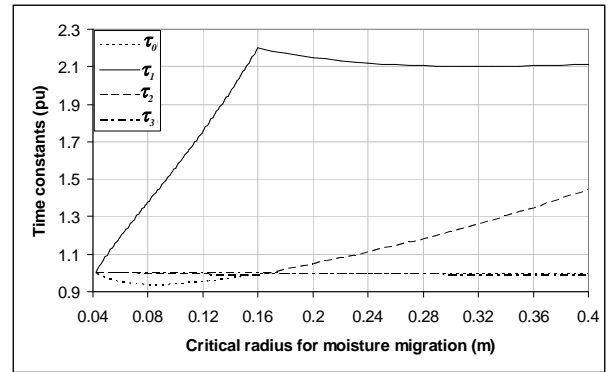


Figure 5: Relation between time constants and the critical radius for moisture migration

Seasonal changes in the prevailing ‘wet’ conditions of the cable environment have a somewhat more linear effect on the time constants and coefficients, and so it is relatively simple to generate continuous functions that relate the effect of ρ_{wet} and r_x on the coefficients and time constants in (1) and (3) from the discrete time constants and coefficients obtained by solving (22) to (41).

The approach is made even more general by coupling external heat sources to the time varying ambient temperature term in (2), as the effect of an external heat source on the hottest conductor can also be approximated by summing exponential terms and rendering them into a real-time formulation. The latter point, however, is not dealt with in this paper.

3.3 The Final Algorithm

The ingredients are now ready for implementation of the transient algorithm incorporating moisture migration and overall seasonal variation. The various methods outlined in the text are summarized in Figure 6.

The upper part of the algorithm need only be performed once for each installation condition, in order to generate the critical radius and wet thermal resistivity dependent functions for the coefficients and time con-

stants of the governing equations. Equation (3) is rewritten below, showing the dependent terms.

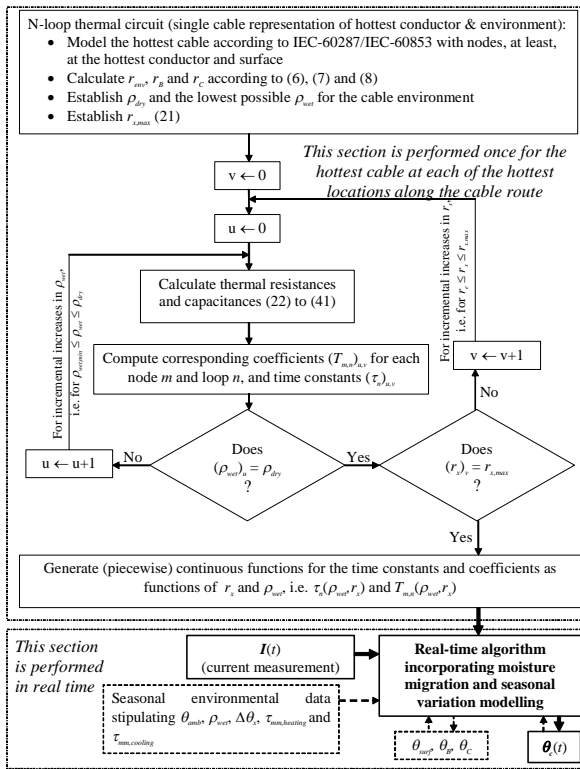


Figure 6: Summary of the methodology culminating in a real-time algorithm with moisture migration modelling and seasonal dependence

$$\theta_{i,j}(t_I) = \theta_{i,j}(t_{I-1}) + [T_{i,j}(\rho_{wet}, r_x) \cdot W_c(\theta_c(t_{I-1})) - \theta_{i,j}(t_{I-1})] \cdot \left[1 - \exp\left(-\frac{(t_I - t_{I-1})}{(\tau_j(\rho_{wet}, r_x))}\right) \right] \quad (42)$$

It is now common practice for modern SCADA systems to perform measurements and calculations every few minutes, in which case the assumption of linearity over one time interval is acceptable. If a time interval of more than a few minutes is envisaged, then the calculations can be based on $(W_c(\theta_c(t_{I-1})) + W_c(\theta_c(t_I)))/2$ with an iterative loop to correct $\theta_c(t_I)$.

Equation (2) coupled with (42) is the main body of the algorithm. This leads us to putting the work developed in this paper to the test, with both simulations and measured data.

4 RESULTS

The test cable installation consists of a 110 kV cable installed in trefoil at a depth of 1.1 m. Each cable has an 800 mm² stranded aluminium conductor, main insulation (XLPE) radius $r_i = 0.035$ m, a lead alloy sheath with outside radius $r_s = 0.0373$ m, and overall radius $r_e = 0.0415$ m. It is permissible, in our opinion, to treat such a cable in one thermal loop, and, as described in this

paper, three loops have been assigned to the environment.

Given that we have based the analysis on a single-phase thermal circuit representation, it might be imagined that trefoil and flat touching installation configurations would stretch the assumptions, due to the lack of radial symmetry as far as one cable in such a configuration is concerned. Nevertheless, the results are surprisingly good. Figure 7 compares the temperature response at the conductor and cable surface predicted by a fastidious FEM simulation, and the real-time algorithm. 2-zone modelling is used in both, with the critical isotherm at 35 °C above ambient, $\rho_{wet} = 1.0$ Km/W and $\rho_{dry} = 2.45$ Km/W. Varying these parameters does not affect the accuracy of the algorithm. There is no delay in either the moisture migration or the moisture return in Figure 7, and the bottom plot shows the movement of the critical radius.

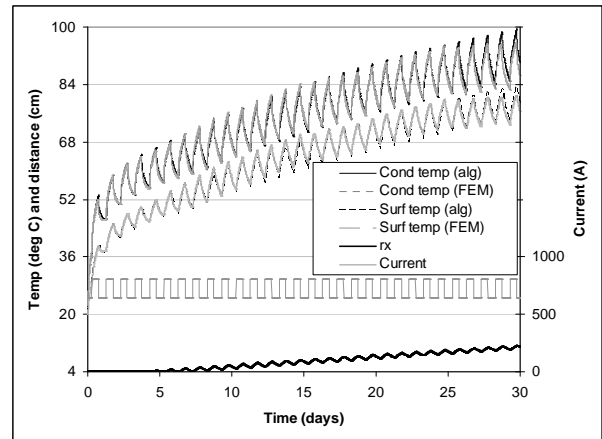


Figure 7: Comparison of a FEM simulation with the responses predicted by the real time algorithm for the conductor and surface temperature of the hottest cable in a trefoil installation. The increase in r_x is also shown.

Figure 7 implies that the logarithmic temperature distribution approximation used for apportioning the thermal capacitances ((9) and (19)) and locating the critical radius for moisture migration (12), and the conversion of a multiphase installation to a single-phase equivalent, are sufficiently valid for multi-cable installations. It is of course interesting to see whether the 2-zone approach to moisture migration is an appropriate model for use in a fully transient application. In order to investigate emergency conditions in a cable-scale setting, we have built a heating tube of outside diameter 70 mm, in a sand back-filled trench. The tube itself is constructed of aluminium, and has a relatively low heat capacity, making it very sensitive to environmental changes. The temperature field on and around the tube is continuously monitored with Pt100 sensors.

Figure 8 shows a period of thermally unstable behaviour in the tube, with measured temperatures alongside the algorithm with no special ‘tuning.’ We use the assumed critical temperature rise of 35 °C above ambient, a wet thermal resistivity of 1.0 Km/W, a dry thermal resistivity of 2.3 Km/W, and the ambient temperature,

measured at a remote location at the same burial depth (1.1 m) rose from 8 to 9 °C during the test period, which was in spring.

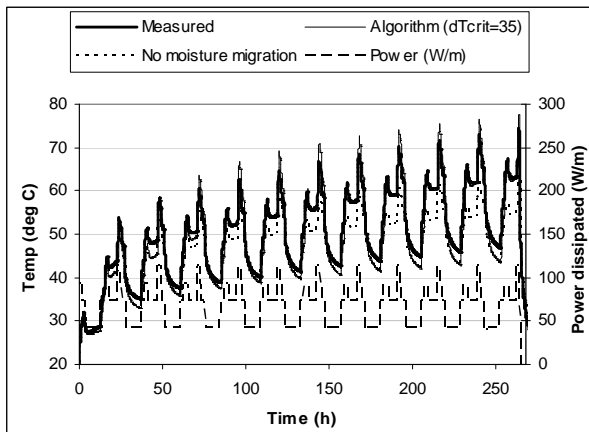


Figure 8: The algorithm vs. reality, measured data from a heating tube in sand backfill

For comparison purposes, a plot of the response with no moisture migration is also shown in Figure 8, showing the importance of having moisture migration modelling in the algorithm.

5 CONCLUSIONS

In order to fully utilise the allowable operating temperatures of modern underground power cables and manage them safely during emergencies, it is imperative that transient rating systems include moisture migration modelling. If specialised backfills are utilised that reduce the risk of moisture migration, allowance should still be made for seasonal variations in the overall cable environment. This paper has outlined an approach that not only copes with moisture migration, but also allows real-time variation of environmental parameters due to seasonal change.

The foundation of the method is to model the temperature rise of a cable by a summation of exponential equations. A method is shown whereby a directly buried cable installation can be represented by a thermal ladder circuit, but even installations that defy analytical treatment can be modelled if the step response, determined by a numerical analysis such as FEM or even measurements, can be approximated by a summation of exponential terms. This is appropriate for the vast majority of cable installations. The real-time formulation of the algorithm allows redefinition of the thermal parameters at every time increment, and so, if the effect of temperature dependent and environmental changes can be mathematically related to the coefficients and algorithms of the governing equations, they can be validly incorporated into the algorithm, as long as the system can be considered linear over one time increment.

The mathematical integrity of the approach was demonstrated by comparison with long-term FEM simulations, which are based on much more rigorous modelling of the cable than the algorithms are.

Using the 2-zone approach for moisture migration in a transient algorithm is of course not perfect, but tests with a heating tube in sand backfill showed that it is good enough for practical purposes. Further, the algorithm can be tuned to allow slower than instantaneous migration of moisture away from the critical isotherm and, more importantly, slower return of the moisture during cooling. The critical temperature for moisture migration is very sensitive to the moisture content, and can also be given a seasonal or rainfall-dependency along with the wet value of thermal resistivity and diffusivity.

REFERENCES

- [1] L. Goehlich, F. Donazzi, R. Gaspari, "Monitoring of HV Cables Offers Improved Reliability and Economy by Means of 'Power Sensors', *Power Engineering Journal*, June 2002
- [2] G.J. Anders, A. Napieralski, M. Zubert, M. Orlikowski, "Advanced modeling techniques for dynamic feeder rating systems", *IEEE Transactions on Industry Applications*, Vol. 39, Issue 3, May-June 2003
- [3] F. de Wild, G. Maijer and G. Geerts, "Extracting More Value with Intelligent Cable Systems", *Transmission and Distribution World*, pp. 22-27, August 2004
- [4] "Calculation of the cyclic and emergency rating of cables. Parts 1 and 2." IEC 60853-1 and 60853-2, 1989.
- [5] G.J. Anders, 1997, *Rating of Electric Power Cables*, IEEE Press Power Engineering Series, McGraw-Hill Book Company, New York
- [6] "Electric cables – Calculation of the current rating," IEC-60287-1-1, 2001
- [7] F.C. Van Wormer, "An improved approximate technique for calculating cable temperature transients," in *Trans. Amer. Inst. Elect. Eng.*, vol. 74, part 3, pp. 277-280, April 1955
- [8] J.H. Neher, "The Transient Temperature Rise of Buried Power Cable Systems," *IEEE Trans. Power App. Syst.*, vol. PAS-83, pp. 102-111, 1964
- [9] G.J. Groeneveld, A.L. Snijders, G. Koopmans and J. Vermeer, "Improved Method to Calculate the Critical Conditions for Drying Out Sandy Soils around Power Cables", *IEE Proceedings*, Vol. 131, Pt. C, No. 2, pp. 42-53, March 1984